Somatic Integration From an Adenoviral Hybrid Vector into a Hot Spot in Mouse Liver Results in Persistent Transgene Expression Levels *In Vivo*

Anja Ehrhardt[1,4], Stephen R Yant[1], Jeffery C Giering[1], Hui Xu[1], Jeffrey A Engler[2] and Mark A Kay[1,3]

[1]*Department of Pediatrics, School of Medicine, Stanford University, Stanford, California, USA;* [2]*Department of Biochemistry and Molecular Genetics, Schools of Medicine and Dentistry University of Alabama at Birmingham, Birmingham, Alabama, USA;* [3]*Department of Genetics, School of Medicine, Stanford University, Stanford, California, USA*

We have developed a hybrid vector that combines the high transduction efficiency of a gene-deleted adenoviral vector and the integration machinery of the bacteriophage-derived integrase ΦC31 for stable transduction and limited integration sites. We based our system on a two-vector system in which the transgene expression cassette is circularized from a helper-dependent vector by Flp-mediated recombination, followed by ΦC31-mediated integration. Integration of the transgene expression cassette from the adenoviral vector resulted in 5-fold higher transgene expression levels in the active ΦC31 group compared to the control group, which received a mutated and inactive version of ΦC31. We confirmed transgene integration into the previously described mpsL1 hot spot of integration by polymerase chain reaction analyses of DNA isolated from mouse livers. In addition, we cloned 40 integration sites. The hot spot mpsL1 was detected only once, and 44% of all integration events were found to be present in gene regions. With further optimization, this system represents a new tool for gene therapy protocols that may offer an alternative to gene therapy approaches based on random integrating viral vectors.

Received 24 April 2006; accepted 13 September 2006.
doi:10.1038/sj.mt.6300011

INTRODUCTION

Successful gene therapy approaches for genetic diseases require sustained and life-long transgene expression levels at a therapeutic range at a non-toxic dose. Integrating viral and non-viral vectors were shown to result in sustained transgene expression levels *in vitro* and *in vivo*, but both delivery systems have advantages and disadvantages. In contrast to non-viral vector approaches, viral vectors usually display high transduction efficiencies of the target cell *in vitro* and *in vivo*, but the humoral response against incoming capsid proteins and cell-mediated immunity remain a major challenge for viral-based gene therapy vector. Furthermore, many virus-based gene transfer approaches are hampered by the risk of insertional mutagenesis. It was shown that retroviral vectors predominantly integrate into active genes[1] and there is strong evidence that integration of recombinant retroviral vector DNA into the host genome was the cause for three leukemia incidences in a human clinical trial for X-linked severe combined immunodeficiency disease.[2,3] Novel adeno-associated virus (AAV) vectors based on various serotypes were shown to result in long-term transgene expression and high transduction efficiencies *in vivo*. However, a small percentage of the stably transduced AAV vector DNA in mouse liver integrate into genomic DNA and most of the integration occurs in active genes.[4]

In sharp contrast to viral-based gene delivery approaches, non-viral vector systems are less immunogenic and are able to stably maintain vector-encoded transgenes. However, efficient delivery of foreign DNA without toxicity and efficient transduction of the target cell remains a major obstacle. Two non-viral vector systems for somatic integration currently used in gene therapy approaches are based on the Sleeping Beauty (SB) transposase or the bacteriophage integrase ΦC31 from *Streptomyces*. SB belongs to the TC1/mariner family of transposable elements and SB-mediated recombination is based on a cut-and-paste mechanism.[5] Recent data from our laboratory demonstrated that sites of insertion after SB-mediated integration are widely distributed but result in a small bias towards genes.[6] In contrast to SB, the bacteriophage integrase ΦC31 recombines DNA for somatic integration in an unidirectional manner. The recombination process is based on a 2-bp staggered cut followed by rotation of the DNA targets by 180°, which results in integration of foreign DNA.[7] One major advantage of the ΦC31 integrase is that this recombinase results in integration into limited "hot spot" sites in the mammalian genome.[8,9] This feature of the ΦC31 integrase would significantly decrease the risk of insertional mutagenesis in a clinical gene therapy setting.

Helper-dependent (HD) adenoviral vectors devoid of all viral coding sequences offer high transduction efficiencies and therapeutic long-term transgene expression levels.[10–13] Various

Correspondence: Mark A Kay, Departments of Pediatrics and Genetics, School of Medicine, Stanford University, Stanford, California 94305, USA.
E-mail: markay@stanford.edu

[4]*Current address: Department of Virology, Max von Pettenkofer-Institute, Ludwig-Maximilians-University of Munich, Munich, Germany.*

studies showed that HD vectors result in a significantly reduced cytotoxic response and long-term phenotypic correction in mouse and rat models.[10,13] After adenoviral transduction, transgene expression levels are initially high but slowly decline over time.[10,14] The loss of vector genomes and transgene expression after adenoviral gene transfer is at least in part due to the episomal nature of adenoviral vector genomes. Hybrid vectors based on adenovirus for efficient gene delivery and stable transgene expression levels were developed,[15–20] but for somatic integration into the host genome, recombinases were used, which have a high risk for insertional mutagenesis. Retroviral hybrid vectors with and without retroviral integrase were generated for stable transduction of target cells, but due to the integration pattern of retroviral vectors there was a high risk of insertional mutagenesis.[15,16] Furthermore adeno-AAV hybrid vectors were generated and integration into the host genome was demonstrated.[17] In a previous study, we generated a gene-deleted adenoviral vector that utilized the SB transposase for stable transgene expression levels *in vivo*.[18] Although we observed stabilized transgene expression levels during rapid cell cycling of mouse hepatocytes, the SB integration machinery still leads to a random integration pattern that may lead to insertional mutagenesis.

For a safer gene therapy protocol, vectors with high transduction efficiencies that utilize alternative integration machineries for site-specific integration without any detrimental effects on the target cell would be advantageous. It was demonstrated that integration mediated by the bacteriophage integrase ΦC31 derived from a Streptomyces phage resulted in integration into hot spots of the host genome by recombining the ΦC31 recognition site attB in an episomal plasmid with pseudo-attP sites in the host chromosome. However, for these non-viral vectors, clinically relevant delivery approaches are still problematic. This study describes the development of a novel hybrid vector that combines high transduction efficiencies of recombinant adenoviral vectors with the best features of the bacteriophage integrase ΦC31 for stable transduction and limited integration sites.

RESULTS

PhiC3-mediated integration efficiencies from circular and linear substrates

Recombinant adenoviral vector genomes mainly persist as linear DNA molecules. Our previous data demonstrated that *Sleeping Beauty*–mediated transposition from a gene-deleted adenoviral vector was more efficient from a circular compared to a linear substrate.[18] This motivated us to first compare the ΦC31-mediated integration efficiencies from circular and linear episomal non-viral DNA. Thus, we performed a colony-forming assay in HeLa cells to determine the integration efficiencies of linear and circular substrates. The same molar amounts of the circular substrate (C)-pCR-attB-Snori and the linear substrate (L)-pCR-attB-Snori that allow for G418 selection *in vitro* were co-transfected into HeLa cells with a ΦC31 encoding plasmid (**Figure 1a**). Control groups received either an inactive version of ΦC31 (m-ΦC31) or "stuffer" DNA co-transfected with the substrates (C)-pCR-attB-Snori or (L)-pCR-attB-Snori, respectively (**Figure 1a**). Fourteen days after selection, a methylene blue staining was performed and cell colonies were counted. We found that the ΦC31 integration efficiency was 14.8-fold higher from circular substrates (**Figure 1b**), and 3.8-fold higher from linear DNA molecules when compared to the mutant integrase control groups (**Figure 1b**). The mechanism involved in low-level ΦC31-mediated integration from linear substrates remains to be determined. In order to improve safety and to avoid integration of the complete linear adenoviral DNA molecule, we based our integrating adenoviral hybrid system on an HD vector in which the transgene expression cassette with the ΦC31 recognition site attB was flanked by the Flp recombinase recognition sites FRT. In the presence of the Flp recombinase, the transgene expression cassette was excised from the adenoviral vector genome to form a circular substrate followed by ΦC31-mediated integration (**Figure 1c**).

Characterization of the novel hybrid vector system for somatic integration *in vitro*

To generate gene-deleted adenoviral vectors that express the bacteriophage integrase ΦC31 and the Flp recombinase, we constructed the plasmid pFTC-INT-Flp (**Figure 2a**). This vector expresses ΦC31 under the control of the Rous sarcoma virus (RSV) promoter and Flp recombinase under the control of the elongation factor alpha-1 promoter. As a control, we generated the vector pFTC-mINT-Flp encoding the inactive version of m-ΦC31. To show the functionality of these plasmid constructs, we performed a colony-forming assay. We co-transfected HeLa cells with the plasmid (C)-pCR-attB-Snori (which allows for G418 selection) with either pFTC-INT-Flp or pFTC-mINT-Flp at a molar ratio of 1:1. Integration efficiencies were 6.2-fold higher for pFTC-INT-Flp compared to the negative control group that received the inactive ΦC31 mutant plasmid (**Figure 2b**).

The HD vector FTC-hFIX-attB-(FRT)2 was used to show *in vitro* efficacy of the adenovirus-integrase hybrid vector (**Figure 3a**). This vector contains a split human coagulation factor IX (hFIX) expression cassette in which the 3′ cDNA of hFIX and the polyA signal are physically separated by part of the first intron of the hFIX gene from the liver-specific human alpha-1-antitrypsin promoter (hAAT-p) and the 5′ cDNA. In addition, this split hFIX expression cassette contains the ΦC31 attachment site, attB, and is flanked by FRT sites for Flp-mediated circle formation from the HD adenoviral vector. The hAAT-p can control transgene expression only if the components of the hFIX expression cassette are excised from the HD vector. Huh7 cells were co-transduced with the vector FTC-hFIX-attB-(FRT)2 and the HD vector FTC-INT-Flp (**Figure 2a**) at a multiplicity of infection (MOI) of 5.5 each. Control groups received the gene-deleted adenoviral vector FTC-TCM without FRT sites and a split hFIX expression cassette to show that transgene activation is dependent on Flp-mediated excision and circle formation (**Figure 3a**). As a positive control for transgene expression, we infected Huh7 cells with the first-generation adenoviral vector fgAdhFIXmg[10] in which the hFIX expression cassette was not split. After circularization, we detected similar hFIX expression levels for the split hFIX expression cassette and the positive control group, which received fgAdhFIXmg with a

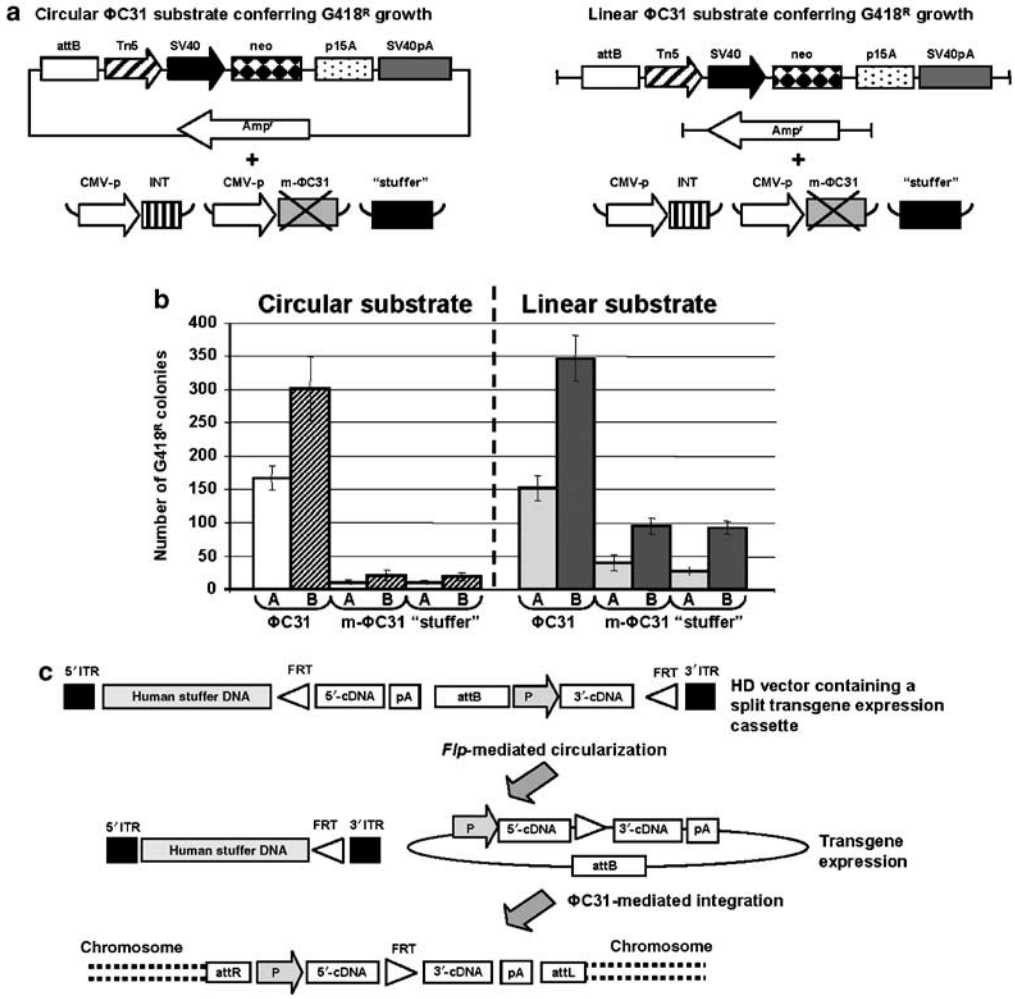

Figure 1 Strategy to develop a gene-deleted adenoviral vector that utilizes the bacteriophage integrase ΦC31 for somatic integration. (**a**) To determine integration efficiencies from circular and linear substrates after ΦC31-mediated integration, a colony-forming assay was performed. The circular substrate (C)-pCR-attB-Snori and the linear substrate (L)-pCR-attB-Snori, which allow for G418 selection *in vitro*, were co-transfected with a ΦC31 encoding plasmid into HeLa cells. Fourteen days after selection, a methylene blue staining was performed and cell colonies were counted. As controls, either an inactive version of ΦC31 (m-ΦC31) or ''stuffer'' DNA was co-transfected. The circular ΦC31 substrate conferring G418-resistant growth contained a neomycin-resistance gene (neo), the p15 bacterial origin of replication (p15A), the simian virus 40 promoter, the Tn5 promoter, and the integrase ΦC31 attachment site attB. The linear substrate was generated by restriction enzyme digest of (C)-pCR-attB-Snori. (**b**) Integration efficiencies from the circular substrate (C)-pCR-attB-Snori and the linear substrate (L)-pCR-attB-Snori determined by a colony-forming assay. The total number of cell colonies per plate was counted. A: 3.8×10^4 cells were seeded per dish; B: 3.8×10^5 cells were seeded per dish. Mean $\pm$ SD is shown ($n = 3$/group). (**c**) Strategy to develop an HD adenoviral vector for somatic integration *in vivo*. For proof of principle, the vector contains a split transgene expression cassette for which transgene expression is dependent on Flp-mediated circle formation. Flp-mediated recombination results in a circular substrate for ΦC31-mediated integration. P, promotor; attB, ΦC31 recognition site; ITR, adenoviral inverted terminal repeat; Flp, Flp recombinase; ΦC31, bacteriophage integrase; pA, polyadenylation signal; attR and attL; hybrid sequences of attB and pseudo-ΦC31 recognition sites in the host genome.

regular hFIX expression cassette (**Figure 3b**). In sharp contrast, transgene expression levels were 10-fold lower in wells that received the HD vector pFTC-TCM without FRT sites (**Figure 3b**), showing that transgene activation was dependent on Flp-mediated excision from the adenoviral vector genome. We speculate that the very low level of detectable hFIX expression in this group may be the result of the formation of circular adenoviral vector genome monomers in which the adenoviral inverted terminal repeats are joined either by homologous recombination or non-homologous end joining because only in the context of this molecular formation can the promoter direct transgene expression.

To further evaluate circle formation, we performed a PCR analysis on DNA isolated from each of the study groups. Primers 1 and 3 detect the HD vector after Flp-mediated recombination and primers 2 and 3 span the FRT site in the gene-deleted adenoviral vector without excision (**Figure 3a**). As expected, we observed excision only in the group that received the adenoviral vector FTC-hFIX-attB-(FRT)2 and not in groups that received either the adenoviral vector FTC-TCM or the first-generation virus fgAdhFIXmg (**Figure 3c**). We detected intact HD vector genomes without Flp-mediated excision only in those cells that received the adenoviral vector FTC-TCM (**Figure 3c**). To show circle formation *in vivo*, we co-delivered 1×10^9 transducing

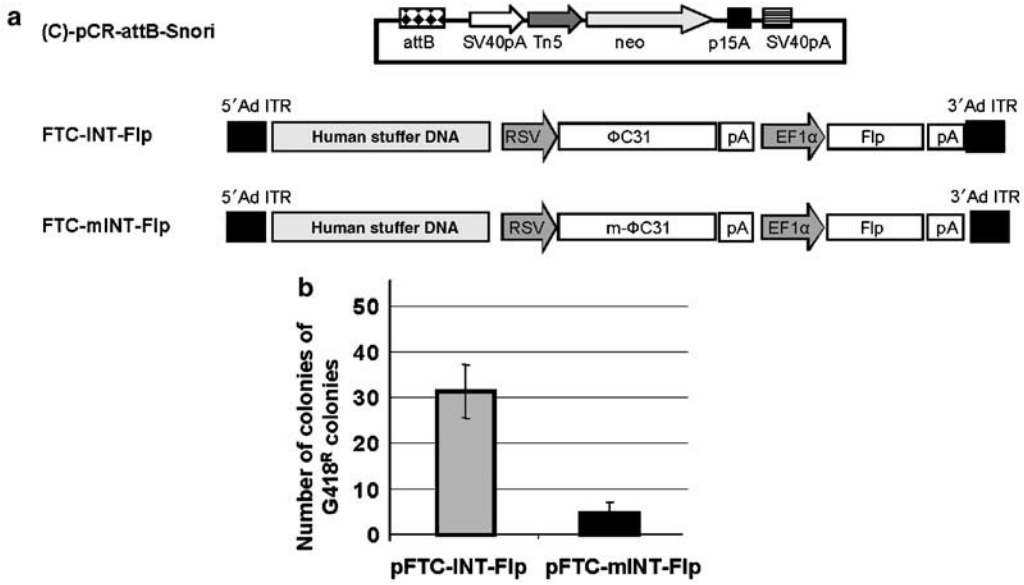

Figure 2 Colony-forming assay to show efficacy of DNA sequences contained in the adenoviral vectors FTC-INT-Flp and FTC-mINT-Flp expressing Flp and either ΦC31 or the mutated version of ΦC31 (m-ΦC31). (**a**) The substrate for ΦC31-mediated integration conferring G418-resistant growth ((C)-pCR-attB-Snori) is depicted on the top and contained a neomycin-resistance gene (neo), the p15 bacterial origin of replication (p15A), the simian virus 40 promoter, the Tn5 promoter, and the integrase ΦC31 attachment site attB. The DNA constructs for adenoviral production (pFTC-INT-Flp and pFTC-mINT-Flp) contained the coding sequence for Flp recombinase (Flp) driven by the elongation factor alpha-1 promoter (EF1α) and an expression cassette for either ΦC31 or the mutated version of ΦC31 (m-ΦC31) under the control of the RSV promoter. (**b**) HeLa cells were co-transfected with the substrate and either the plasmid pFTC-INT-Flp or pFTC-mINT-Flp at a molar ratio of 1:1, respectively. Cells were selected for 2 weeks, methylene blue staining was performed, and blue-forming units were counted. Groups were performed in triplicate. Mean ± SD is shown ($n = 3$/group).

units (TU) of the HD vector FTC-hFIX-attB-(FRT)2 (**Figure 3a**) and 1×10^9 TU of the second HD vector FTC-INT-Flp encoding Flp and ΦC31 (**Figure 2a**). Genomic DNA was isolated and excision of the split transgene expression cassette from the gene-deleted adenoviral vector was detected by PCR (**Figure 3d**).

The adeno-ΦC31 hybrid vector results in sustained transgene expression levels *in vivo*

To establish functionality *in vivo*, we used a combination of two adenoviral vectors. C57Bl/6 mice ($n = 4$) were coinjected with 1×10^9 TU of the HD vector FTC-hFIX-attB-(FRT)2 (**Figure 3a**) and 1×10^9 TU of the second HD vector FTC-INT-Flp that expressed the two recombinases Flp and ΦC31 (**Figure 2a**). Control mice received the HD vector FTC-mINT-Flp (**Figure 2a**), which encodes Flp and the inactive version of ΦC31. We obtained supra-physiological serum levels of hFIX (up to 54,000 ng/ml, normal level = 5,000 ng/ml) 7 weeks post-injection (**Figure 4a**). In sharp contrast, mice infused with the HD vector containing a split hFIX expression cassette without FRT sites resulted in serum hFIX levels of up to 1,700 ng/ml, establishing Flp-mediated transgene activation. To evaluate *in vivo* integration of the vector, we induced rapid cell cycling in mouse livers, a process known to eliminate over 95% of episomal genomes (**Figure 4a**). We observed no significant differences between groups that received ΦC31 or the mutated version of ΦC31 and this indicated that ΦC31 expression in the context of this gene-deleted adenoviral vector was not sufficient to detect somatic integration by hFIX expression levels. Limited toxicity studies revealed that there was a slight elevation of liver enzymes 1 day post-injection, as demonstrated by serum glutamic pyruvic transaminase (SGPT) levels (**Figure 4b**). We concluded that one reason for this result might have been that ΦC31 expression levels were not high enough for efficient somatic integration of the transgene or that the molar ratio of the transgene expression cassette and the ΦC31 and Flp encoding vector was not sufficient to get measurable integtation. We reasoned that one way to optimize the experiment would be to change the ratio of transgene and Flp and ΦC31 encoding vectors and to simply increase the copy numbers of Flp and ΦC31 encoding DNA. It is well established that hydrodynamic tail injection results in efficient transduction of up to 40% of all hepatocytes with up to 60 copies per cell even 2 months after injection.[21] A significant increase in the dose of the gene-deleted adenoviral vector encoding for Flp and ΦC31 most likely would have resulted in transient toxicity and may not have resulted in sufficient ΦC31 expression levels.

Thus, in our second approach, we performed a study in C57Bl/6 mice in which a ΦC31 and Flp encoding DNA plasmid was administered into mouse liver by high-pressure tail-vein injection (**Figure 5a**). Four hours later, this step was followed by injection of 5×10^9 TUs of the HD vector FTC-hFIX-attB-(FRT)2 (**Figure 3a**) with the split hFIX expression cassette ($n = 5$ per group). Control mice received a plasmid encoding the inactive version of ΦC31 (m-ΦC31). At day 52 post-injection, we measured serum hFIX levels of up to 3,000 ng/ml in both groups (**Figure 5b**). To confirm integration, we induced rapid cell cycling of mouse hepatocytes by injecting CCl_4 intraperitoneally. With this approach, we observed a 5-fold difference in serum hFIX levels between the active ΦC31 and the inactive m-ΦC31 control group, 122 days post-injection (**Figure 5b**). At this time,

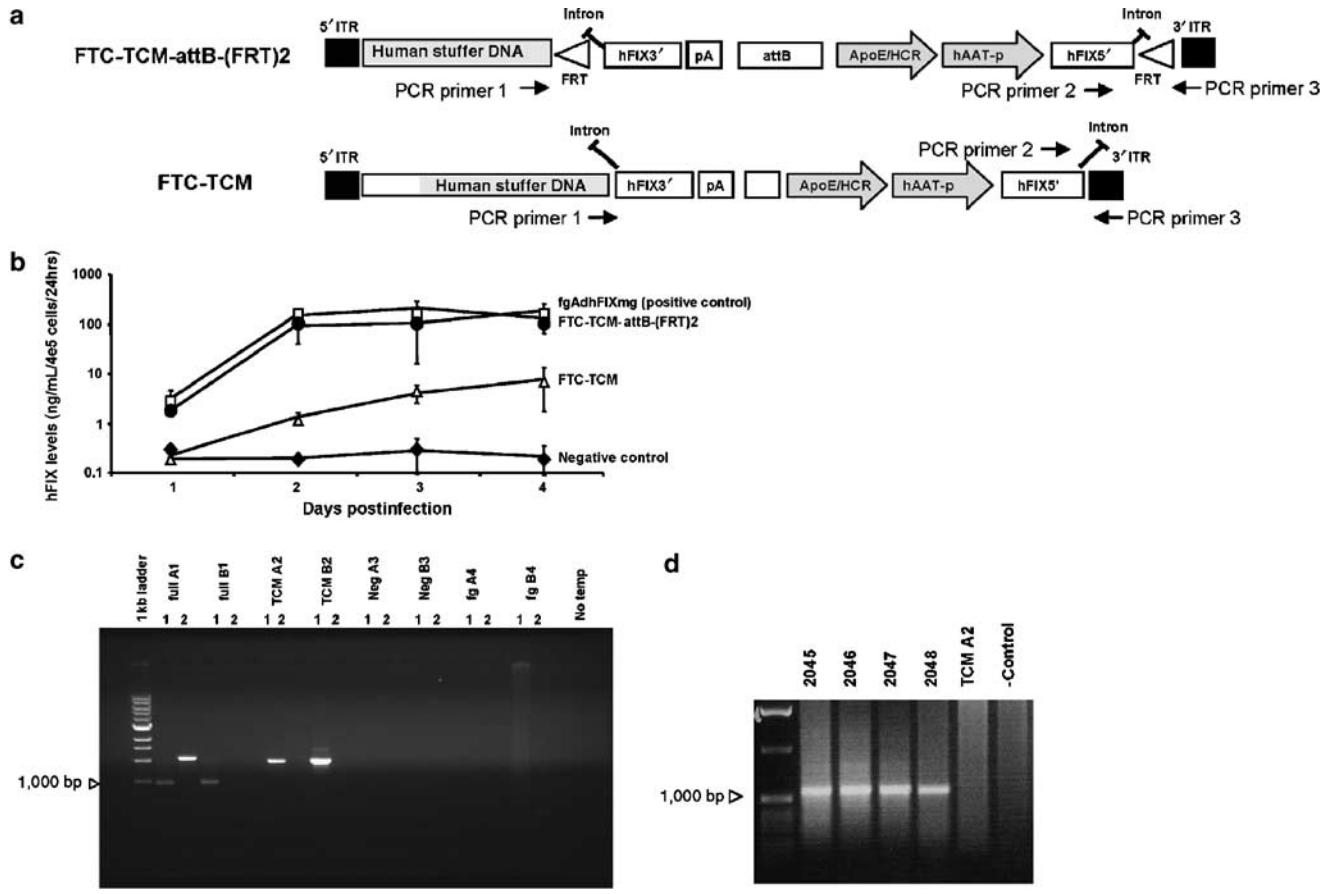

Figure 3 Characterization of the adeno/ΦC31 hybrid vector *in vitro*. (**a**) DNA sequences in the adenoviral vector genomes used for the *in vitro* studies. The gene-deleted adenoviral vector FTC-TCM-attB-(FRT)2 contained an hFIX expression cassette in which part of the hFIX coding sequence is physically separated from the liver-specific hAAT-p and the two liver-specific enhancers: the hepatocyte control region (HCR) and the apolipoprotein E (ApoE) enhancer sequence. The 3′ and the 5′ ends of the hFIX coding sequence are separated by the 1.4-kb truncated intron A from the hFIX gene. Only if circle formation from the adenoviral vector occurs, transgene expression will be activated. The control vector FTC-TCM is lacking FRT sides for Flp-mediated recombination. AttB, ΦC31 recognition site; ITR, adenoviral inverted terminal repeat; pA, polyadenylation signal. (**b**) Flp-mediated excision of the split hFIX expression cassette results in activation of transgene expression *in vitro*. Six-well plates with Huh7 cells were coinfected with the vector FTC-INT-Flp and either the vector FTC-TCM-attB-(FRT)2 or the vector FTC-TCM without FRT sites. Control groups received either a first-generation adenovirus fgAdhFIXmg[10] with an hFIX expression cassette as a positive control or no adenoviral vector as a negative control. For all groups, a total MOI of 11 was used. Transgene expression levels were periodically measured by ELISA detecting hFIX expression levels in the supernatant of Huh7 cells. Mean ± SD is shown ($n = 3$/group). (**c**) Flp-mediated excision of the split hFIX expression cassette. On day 4 post-transduction, genomic DNA from all four groups depicted in **b** was isolated and a PCR with two different primer pairs was performed. Primer pair 1 combines primers 1 and 3 (depicted as horizontal arrows in **a**) and results in a 1-kb band if excision occurred. Primer pair 2 combines primers 2 and 3 (shown as horizontal arrows in **a**), which span the FRT site close to the 3′ ITR. This primer pair detects the adenoviral genomes FTC-TCM-attB-(FRT)2 and FTC-TCM without excision. 1, primer pair 1; 2, primer pair 2. (**d**) PCR to show Flp recombinase–mediated excision from the gene-deleted adenoviral vector FTC-TCM-attB-(FRT)2 *in vivo*. The HD vector FTC-TCM-attB(FRT)2 containing the split hFIX expression cassette was co-delivered into C57Bl/6 mice ($n = 4$; mouse numbers 2,045–2,048) with the Flp- and ΦC31-expressing HD vector FTC-INT-Flp. Genomic DNA was isolated and to detect Flp-mediated excision a PCR with primer pair 1 was used. Control mice received an irrelevant adenoviral vector and as another negative control we added genomic DNA from TCM A2 as shown in **c**.

serum hFIX levels were still within the therapeutic range (up to 600 ng/ml or 12% of normal). This observation was in concordance with the total vector genome copy number in mouse livers 122 days post-injection, which were 5-fold higher in the ΦC31 group compared to the m-ΦC31 group (**Figure 5c**), as determined by quantitative real-time PCR.

Integration site analysis after ΦC31-mediated integration of the transgene expression cassette from the gene-deleted adenoviral vector into the host genome

In order to begin to identify sites of DNA insertion in mouse liver after ΦC31-mediated integration, we used an established PCR approach (**Figure 6a**). We detected the previously described hot spot of integration mpsL1 on mouse chromosome 2, band H3, in all mouse livers ($n = 3$) that received the HD vector FTC-hFIX-attB-$(FRT)_2$ and the active bacteriophage integrase (**Figure 6a**). In sharp contrast to this observation, there was no PCR product specific for the hot spot mpsL1 in mouse livers ($n = 4$) that were infused with the HD vector FTC-hFIX-attB-(FRT)2 and the inactive m-ΦC31 integrase (**Figure 6a**). Detailed characterization of PCR products specific for mpsL1 revealed that ΦC31-mediated integration resulted in micro-deletions of up to 6 bp at the attB arm and up to 20 bp at the chromosomal arm (**Figure 6b**).

To determine the overall distribution of integration sites, a modified version of the BD GenomeWalker™ Kit from BD

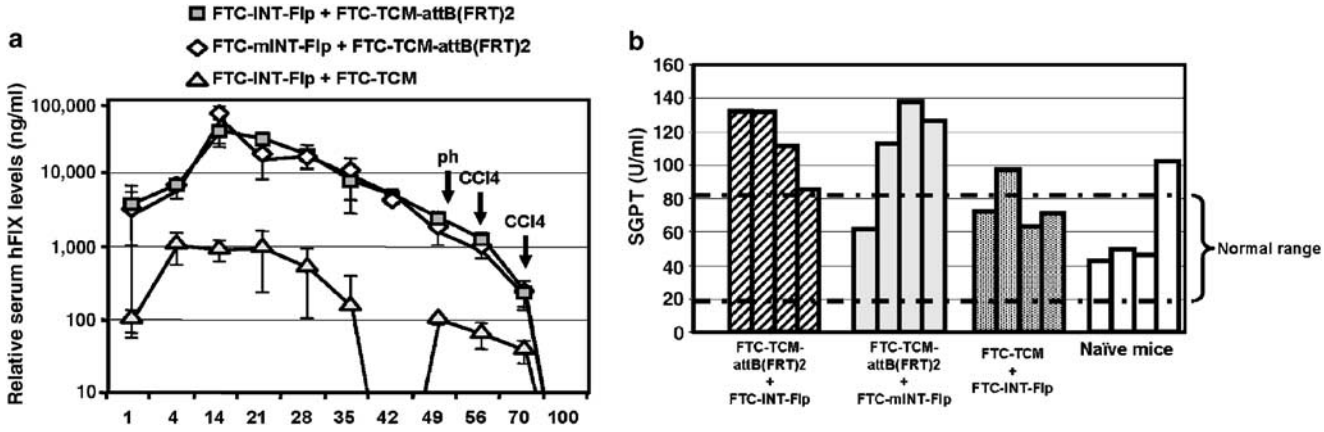

Figure 4 Co-delivery of the gene-deleted adenoviral vector with the split hFIX expression cassette and the Flp recombinase and ΦC31- or m-ΦC31-expressing HD vector, respectively. (**a**) The HD vector FTC-TCM-attB(FRT)2 containing the split hFIX expression cassette was co-delivered with either the Flp- and ΦC31-expressing HD vector FTC-INT-Flp or the Flp- and m-ΦC31-expressing HD vector FTC-mINT-Flp. Control mice received the HD vector FTC-TCM containing the split hFIX expression cassette without FRT sites and the gene-deleted adenoviral vector FTC-INT-Flp. For each adenoviral vector, a dose of 1×10^9 TU was injected, which equaled a total dose of 2×10^9 TU per mouse. Serum samples were obtained periodically by retro-orbital bleeding and an ELISA was performed. To induce cell cycling of mouse hepatocytes *in vivo*, we performed a surgical two-third partial hepatectomy (ph) and we injected CCl_4. Mean ± SD is shown ($n = 3$/group). (**b**) SGPT levels from single mice 1 day post-injection. Serum samples from all three experimental groups were obtained for colorimetric determination of SGPT levels. As a negative control, regular C57Bl/6 mice (naïve mice) were added. Mean ± SD is shown ($n = 4$/group).

Biosciences Clontech (Palo Alto, CA) was used. To avoid potential unknown biases for detection of integration sites, we created four genomic DNA libraries and we analyzed a total of 40 integration sites in mouse livers that received the HD vector FTC-hFIX-attB-(FRT)2 and the active version of the bacteriophage integrase ΦC31. Out of 40 integration sites, 34 were mapped on various chromosomes (**Figure 7**) and although the hot spot of integration, mpsL1, was detected in all analyzed mouse livers using a PCR specific for mpsL1 (**Figure 6a**), this site was found only once in the 40 analyzed sites. We found that 15 out of the 34 mapped integration events from the HD vector landed in genes (44.1%), 15 integration sites (44.1%) were found to be intergenic, and 11.7% (4 out 17) of the integration events were in repetitive elements of the mouse genome (all sites of insertion are described in **Figure 8**). Out of the 15 identified integration events in genes, 13 were detected in introns, two transgenes landed in exons, whereas no insertion into an untranslated region was found. In sharp contrast to these findings, 94% of all analyzed integration sites (15 out 16 sites of insertion) in control livers that received m-ΦC31 and the HD vector FTC-hFIX-attB-(FRT)2 had an intact TTG core, indicating that random integration occurred (not shown).

DISCUSSION

We describe a new vector system in which integration from the gene-deleted adenoviral vector was mediated by the ΦC31 bacteriophage integrase. We demonstrate that this approach results in prolonged transgene expression *in vivo* even after rapid cell cycling.

Although integration efficiencies were significantly higher from circular substrates, we observed that both supercoiled and linearized DNAs were suitable substrates for recombination between attP and attB in mammalian cells (**Figure 1b**). Currently, we can only speculate about the mechanism involved in ΦC31-mediated integration from linear fragments. One possibility would be that double-stranded linear DNA in the cell is converted into circular DNA molecules by non-homologous end joining. One might also speculate that ΦC31 integrase is involved in the formation of circular DNA for integration. Linear DNA fragments can indeed serve as substrates for ΦC31-mediated recombination between attP and attB[22] in bacteria. In an earlier study, we found that SB-mediated integration was not sufficient to mediate transposition from a linear substrate.[18] However, there are fundamental mechanistic differences in the integration process between SB and the bacteriophage integrase ΦC31. In contrast to ΦC31, which works by a 2-bp staggered break followed by integration of the complete DNA fragment, the SB transposase works by a cut-and-paste mechanism.

We based our integrating adenoviral hybrid system on an HD vector in which the transgene expression cassette with the ΦC31 recognition site attB is flanked by the Flp recombinase recognition sites FRT. In the presence of the Flp recombinase, the transgene expression cassette is excised from the adenoviral vector genome to form a circular substrate followed by ΦC31-mediated integration. One reason for this strategy was that ΦC31-mediated integration efficiencies were higher from circular substrates compared to linear substrates. However, low-level random integration of linear adenoviral vector genomes was demonstrated[23] and a recent report described homologous recombination of adenoviral DNA sequences and endogenous sequences in mouse embryonic stem cells.[24] Random integration of recombinant viral vector DNA may present a safety concern for our system. Therefore, excision of the transgene from the adenoviral vector followed by ΦC31-mediated integration may decrease random integration of the complete linear adenoviral DNA molecule into the host genome

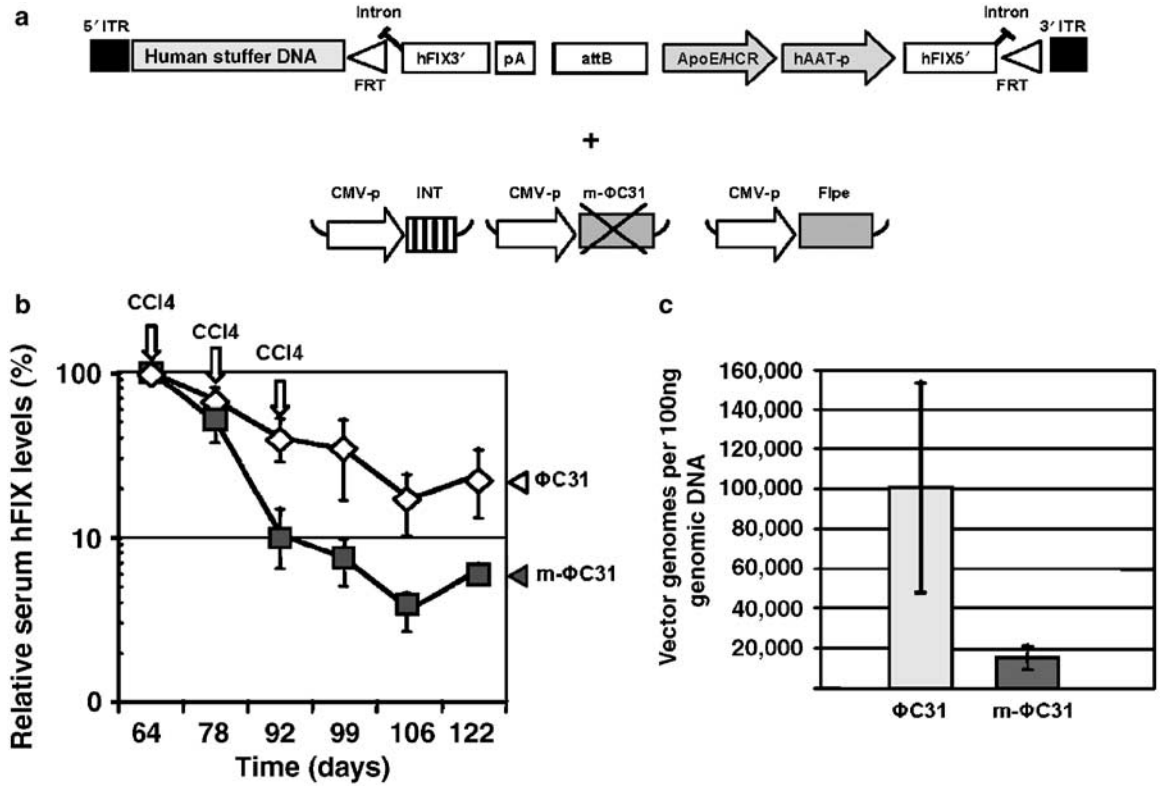

Figure 5 The adeno-ΦC31 hybrid vector results in sustained hFIX expression levels *in vivo*. (**a**) DNA sequences in the HD vector FTC-TCM-attB-$(FRT)_2$ to analyze transgene persistence *in vivo* after ΦC31-mediated somatic integration from the HD vector. ApoE/HCR, two liver-specific enhancers: the hepatocyte control region (HCR) and the apolipoprotein E (ApoE) enhancer; hAAT-p, human alpha-1-antitrypsin gene promoter; hFIX, human coagulation factor IX cDNA with the 1.4-kb truncated intron A from the hFIX gene; attB, ΦC31 recognition site; ITR, adenoviral inverted terminal repeat. Other DNA sequences contained in the gene-deleted adenoviral vector were based on the previously described HD vector pAdFTC.[10] (**b**) Mice ($n = 4$ per group) were sequentially injected with 5×10^9 TU of the HD adenoviral vector FTC-TCM-attB-$(FRT)_2$ and 20 μg Flp and ΦC31 encoding DNA sequences. Control groups received a mutated and inactive version of ΦC31 (m-ΦC31). Relative serum hFIX levels in mice undergoing rapid hepatic cell cycling after CCl_4 injections were monitored by ELISA. Mean $\pm$ SD is shown. (**c**) Total vector genome copy numbers in mouse livers ($n = 3$ per group) 122 days post-injection were determined by a quantitative real-time PCR. Mean $\pm$ SD is shown.

and with regard to gene therapy it may improve safety of this novel vector system.

After *in vivo* delivery of our new adenoviral hybrid vector utilizing ΦC31 for somatic integration, we were able to detect the previously described hot spot of ΦC31-mediated integration mpsL1 in all mouse livers as demonstrated by an established PCR protocol.[25] This finding is in concordance with previous studies in which the same hot spot was detected in mouse liver after non-viral delivery of the ΦC31 integration machinery.[9,25] Furthermore, we were interested in the overall distribution of all integration sites *in vivo*. We were able to identify and characterize a total of 40 sites of insertion in mouse liver after ΦC31-mediated integration. Out of these 40 integration events, we recovered the hot spot mpsL1 in mouse liver once. This finding may indicate that the bacteriophage integrase ΦC31 may be less specific than originally thought. This finding is in concordance with a recent study demonstrating that there are more varied hot spots in various cell types *in vitro*.[26] There is one previous report in which a total of two sites of integration were recovered from mouse liver by nested inverse PCR in a non-viral gene therapy approach and the predominant site of insertion was mpsL1.[9] We believe that there may be several reasons for these differences between our study and the historical data. First of all, integration site selection may be different in a non-viral gene therapy approach compared to a viral gene transfer system. Our strategy was based on ΦC31-mediated integration from a gene-deleted adenoviral vector in which the adenoviral vector contained the transgene and two non-viral vectors encoding for ΦC31 and Flp recombinase. It may be possible that ΦC31-mediated integration combined with adenoviral transduction of hepatocytes and coexpression of Flp recombinase in the target cell might have caused a different integration pattern compared to a non-viral approach. Another explanation for the less specific integration pattern observed in this study may be the strategy chosen to determine integration sites.

We performed a detailed characterization of sites of insertion and found that 44.1% of all rescued sites of insertion were in genes. Furthermore, we found the same percentage (44.1% of all sites of insertion) of integrated transgenes in intergenic regions. A recent study in which an extensive analysis of sites of insertion *in vitro* was performed also showed a small bias toward integration into genes.[26]

This feature of our adeno-integrase hybrid system may represent fundamental advantages compared to other integrating viral vector systems that utilize recombinases or integrases that predominantly target genes. However, with respect to integration

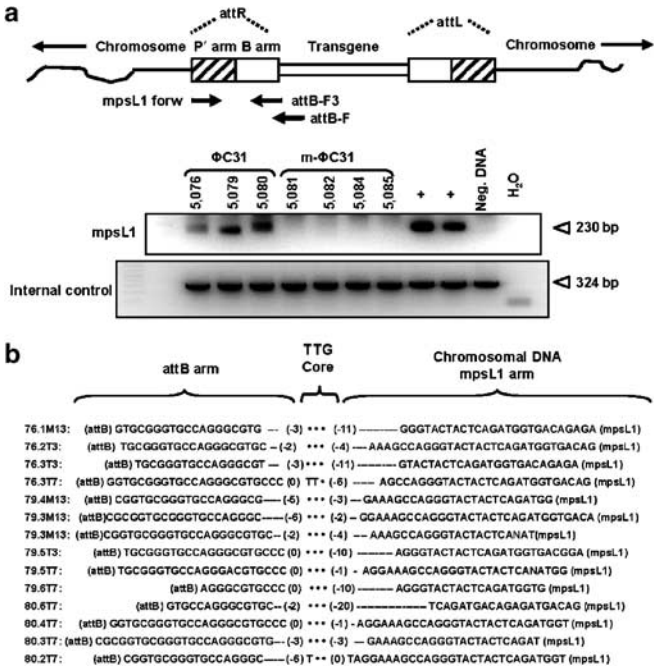

Figure 6 Detailed characterization of sites of insertion into the hot spot mpsL1 in mouse liver after ΦC31-mediated integration from a gene-deleted adenoviral vector. (**a**) The hot spot of integration mpsL1 on chromosome 2 was detected by nested PCR (top panel). The primer binding sites were in the chromosomal mpsL1 site and the attB arm. Genomic mouse liver DNA was isolated and a PCR performed (bottom panel). Primers are schematically shown as horizontal arrows. (**b**) Summary of micro-deletions in chromosomal DNA at the hot spot mpsL1 and the attB arm after ΦC31-mediated integration.

into genes, these characteristics are similar to the integration pattern of the SB transposase.[6]

Various adenoviral hybrid vectors for somatic integration were generated in the past. In sharp contrast to our novel integrating adenoviral hybrid vector, these previously published reports utilized recombinases and integrases with an integration pattern that may result in insertional mutagenesis. Thus, our vector system provides the important advantage of limited integration site selection and with further optimization we believe that this novel integrating adenoviral system presented in this study will significantly reduce the risk of insertional mutagenesis. There was one recent report introducing a gene-deleted adenoviral vector that utilized the Rep68/78 protein from AAV for integration into the natural integration site AAVS1 on human chromosome 19.[27] However, there is strong evidence that Rep proteins are toxic to the cell. In addition, the integration efficiencies of this system in human cells remain to be determined.

Further studies need to address the possibility to create a hybrid vector system in which the bacteriophage recombinase ΦC31 encoding expression cassette, the Flp recombinase encoding DNA, and the transgene with the attB site are encoded by one-gene-deleted adenoviral vector. A ratio of 1:1 (substrate:ΦC31) in a non-viral approach resulted in efficient integration of foreign DNA into the host genome, but a ratio of 1:1 using a two-vector system based on adenovirus did not result in measurable integration efficiencies. An inducible system in which the ΦC31 integrase is expressed under the control of an inducible promoter might be advantageous because long-term expression of the ΦC31 integrase might result in unwanted events. With further improvements of recombinases or other proteins that offer site-specific integration, it may be possible to generate in future a hybrid vector system that lessens the risk of insertional mutagenesis.

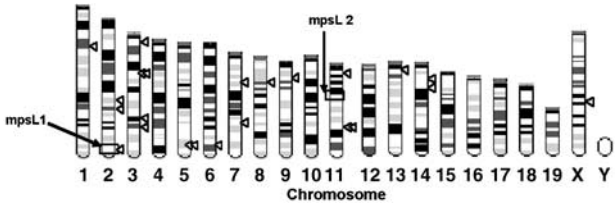

Figure 7 Distribution of sites of insertion after ΦC31-mediated integration from a gene-deleted adenoviral vector in mouse liver. Mapped integration sites are depicted by arrows and the two previously described hot spots of integration, mpsL1 and mpsL2, are marked by a square. The BD GenomeWalker™ Kit from BD Biosciences Clontech was adopted to determine sites of insertion. Four genomic DNA libraries with restriction enzyme endonucleases that create blunt-ended DNA fragments (*Dra*I, *Eco*RV, *Pvu*II, *Ssp*I) were produced and a linker was ligated to the DNA fragments. A two-step PCR was performed in which one primer binds to the attB arm and the other primer binds to the linker (primer pair for first PCR: AttB-F, 5′-tac cgt cga cga tgt agg tca cgg tc-3′ and adopter primer 1 (AP1), 5′-gta ata cga ctc act ata ggg c-3′; primer pair for the nested PCR: AttB-F3, 5′-cga agc cgc ggt gcg-3′ and adopter primer 2 (AP2), 5′-act ata ggg cac gcg tgg t-3′). PCR products were subcloned and DNA sequences analyzed.

MATERIALS AND METHODS

DNA constructs for generation and production of adenoviral vectors. The gene-deleted adenoviral vector pAdFTC[10] and the split hFIX expression cassette[18] were described previously. Instead of the inverted repeats for SB-mediated transposition, this split hFIX expression cassette contained the ΦC31 recognition site attB for ΦC31-mediated integration between the liver-specific promoter and the polyA signal. This split hFIX expression cassette contains a liver-specific promoter, the first exon of the hFIX coding sequence, and part of the first intron of the hFIX gene. These DNA sequences are physically separated from the 3′ end of the first intron of the hFIX gene, the 3′ end of the hFIX coding sequence, and the polyA signal. The split FIX expression cassette was flanked by the Flp recognition sites FRT and all DNA sequences were cloned into the plasmid pAdFTC to generate pFTC-hFIX-attB-(FRT)2. A physical map of this vector is depicted in **Figure 3a**. The gene-deleted adenoviral vector with the identical transgene expression cassette but without FRT sites was called FTC-TCM. Further details about the cloning strategy can be obtained upon request. The plasmids pFlp, pCMV-INT, and pCMV-mINT were described elsewhere.[25,28] Briefly, expression of Flp recombinase, ΦC31, and the mutated and inactive version of the bacteriophage integrase was driven by the cytomegalovirus promoter. To generate the HD vectors pFTC-INT-Flp and pFTC-mINT-Flp for adenoviral production, we ligated *Spe*I/*Bam*HI fragments from pCMV-INT and pCS-mINT into the *Nhe*I/*Bgl*II sites of pRSV-mcs-BpA resulting in the vectors pRSV-INT and pRSV-mINT. In order to obtain the plasmids pHD-Flp-INT and pHD-Flp-mINT, we inserted the *Xho*I/*Ssp*I fragments from pRSV-INT and pRSV-mINT into the *Sma*I and *Bsm*I sites of pHD-SB-Flp-Δ*Not* by blunt-end ligation. To generate the vectors pFTC-INT-Flp and pFTC-mINT-Flp for adenoviral production, the *Pac*I/*Pme*I fragments from pHD-Flp-INT and pHD-Flp-mINT were cloned into the *Pac*I/*Pme*I site of pAdFTC.

Adenoviral vector production. HD adenoviral production was based on a recently published system.[29] In brief, to release the plasmid

Clone ID	[attB]	Mouse chromomsome (Chr) (bp start-bp stop on mouse contig)	Site of insertion
1. D76-1B	−23	Many hits, repetitive element	n/a
2. D76-2C	−2	Chr18 band D3 [53019925-53020162 on NT_039674]	intergenic
3. D76-2F	−26	Chr6 band G2 [3322813-3323555 on NT_039360] Mm6_39400_35	Gene, intron, Gene predicted by Gnomon on Mus musculus C57BL/6J genomic contig
4. D76-3B	−22	Many hits, repetitive element	n/a
5. D76-3E	−4	Chr7 [no hit in mouse genome] ‡	n/a
6. D76-3F	−4	Many hits:	
		Chr2 band H4 [2557016-2556225 on NT_10890]	Gene, intron, LOC620832, similar to ribosomal protein S8
		Chr2 band H4 [51948-52739 on NT_078355]	Gene, intron, LOC620832, similar to ribosomal protein S8
		Chr2 band H4 [179345-180136 on NT_078355]	Intergenic
		Chr2 band H4 [280948-280157 on NT_078355]	Intergenic
		Chr2 band H4 [378509-377718 on NT_078355]	Gene, intron, LOC620832, similar to ribosomal protein S8
		Chr2 band H4 [577552-576761 on NT_078355]	Intergenic
		Chr2 band H4 [796396-795605 on NT_078355]	Intergenic
		Chr2 band H4 [976476-975685 on NT_078355]	Gene, intron, RIKEN cDNA 6230416C02 gene
		Chr2 band H4 [1121017-1120226 on NT_078355]	Intergenic
		Chr2 band H4 [1249086-1248295 on NT_078355]	Gene, intron, LOC621067, similar to gonadotropin inducible ovarian transcription factor 2
		Chr2 band H4 [1406343-1407134 on NT_078355]	Intergenic
		Chr2 band H4 [1701900-1701109 on NT_078355]	Intergenic
		Chr2 band H4 [1897754-1896963 on NT_078355]	Intergenic
		Chr2 band H4 [2895747-2894959 on NT_078355]	Gene, intron, LOC620832, similar to ribosomal protein S8
		Chr2 band H4 [2158-2949 on NT_039212]	Intergenic
		Chr2 band H4 [159081-158291 on NT_039212]	Intergenic
		Chr2 band H4 [285879-285089 on NT_039212]	Gene, intron, LOC621668, similar to zinc finger protein 124
7. D76-3G	0	Chr11 [no hit in mouse genome] ‡	n/a
8. P76-4E	−10	Chr11 band A1 [8253065-8252756 on NT_039515]	Gene, intron, zona pellucida binding protein
9. P76-5E	−5	Chr12 [139291-139786 on NT_114995]	Intergenic
10. D79-7G	−26	Chr17 band B2 [5170636-5171232 on NW_001030618]	Intergenic
11. D79-8C	0	Chr9 band 9c [11586638-11585967 on NT_039474]	Gene, intron, caseinolytic protease X
12. D79-8D	−33	Many hits, repetitive element	n/a
13. D79-9F	−1	Many hits, repetitive element	n/a
14. P79-11G	−12	Chr3 band G1 [23726532-23727060 on NT_039240]	Intergenic
15. P79-11H	−4	Chr14 band B [17414137-17414748 on NT_039606]	Intergenic
16. P79-12B	−4	Chr6 band G1 [5184226-5184785 on NT_039359]	Intergenic
17. P79-12C	0	Chr13 band A1 [2394888-2394465 on NT_039578]	Gene, exon, GLI-Kruppel family member GLI3
18. E79-8C	−13	Chr12 [139766-139391on NT_114995]	Intergenic
19. E79-8F	−15	Chr9 band 9D [68469541-68469264 on NW_001030907]	Intergenic
20. E79-8G	−2	Chr1 band C1.2 [32682612-32682027 on NT_039170]	Intergenic
21. E79-9A	−13	Chr 7 band 7F1[37795526-37796422 on NT_039433]	Gene, intron, dynein, axonemal, heavy chain 3
22. E79-9B	−5	Chr11 [no hit in mouse genome] ‡	n/a
23. S76-4H	−9	Chr10 band C1[3818939-3818577 on contig NT_039500.5]	Intergenic
24. S76-6E	0	Chr19 band 19A [9886892-9886409 on NT_039687.5]	Intergenic
25. S76-11B	−25	Chr2 band 2E5 [30277152-30277557 on NT_039207.5]	Gene, exon, similar to kinesin-like motor protein C20orf23
26. D76-1Br	−6	Chr5 band G1.3 [2135511-2135950 on NT_039314.5]	Gene, Intron, autism susceptibility candidate 2-like isoform 1
27. D76-1Gf	0	Chr3 band G2 [31383774-31383307 on NT_039240.5]	Gene, intron, caspase 6
28. D76-2F	−5	Chr9 band 9D [21137147-21137647 on NT_039474.5]	Intergenic
29. D76-3Br	−3	Chr8 [no hit in mouse genome] ‡	n/a
30. D76-3Gf	−3	Chr5 [no hit in mouse genome] ‡	n/a
31. D76-5Af	−2	Chr12 [40628775-40628278 on NT_039551.5]	Intergenic
32. D76-5Ef	−2	ChrX band XC2 [109674-109132 on NT_039711.4]	Gene, Intron, Cdc42 guanine nucleotide exchange factor (GEF) 9 isoform 7, Cdc42 guanine nucleotide exchange factor (GEF) 9 isoform 2
33. D76-5Hr	−3	Chr2 band 2E3 [23964365-23965080 NT_039207.5]	Intergenic
34. D79-9Fr	−2	Chr8 band 8A3 [29149429-29150039 on NT_039455.5]	Gene, intron, RNA binding protein gene with multiple splicing isoform 1
35. D76-8	−1	Chr7 band 7B3 [1547484-1547908 on NT_039420.5]	Gene, intron, hypothetical protein LOC75510 isoform 1
36. P79-12D	−23	Chr14 band 14B [8441326-8440680 on NT_039606.5]	Gene, intron, glutamate receptor, ionotropic, delta 1
37. D76-3Cf	−24	Chr9 band 9A4 [16342987-16343647 on NT_039472.5]	Gene, intron, neurotrimin
38. D76-3Ff	−2	ChrX [no hit in mouse genome] ‡	n/a
39. D76-5Gf	−2	Adenovirus type 2, 5'ITR [1-455]	n/a
40. D76-1	−33	Chr11 band 11B4 [40957157-40958088 on NT_096135.3]	Gene, intron, serine (or cysteine) proteinase inhibitor, clade F, member 1

‡NCBI Blast of the mouse genome gave no hit; DNA sequence not mapped and therefore no further information about the characteristics of this site of insertion available.

Figure 8 Detailed description of sites of insertion in mouse liver. Listed are all 40 sites of insertion. Nucleotide deletions in the attB arm and the nucleotide numbers of the subcloned and sequenced chromosomal DNA on the contig are given. Information about hits in genes and integenic regions is provided. ‡NCBI Blast of the mouse genome gave no hit; DNA sequence was not mapped and therefore no further information about the characteristics of this site of insertion was available.

backbone, the plasmids pFTC-hFIX-attB-(FRT)2, pFTC-INT-Flp, and pFTC-mINT-Flp were linearized by *Not*I digest and transfected into 116 cells,[29] which stably express Cre recombinase, using Superfect tranfection reagent (Qiagen, Valencia, CA). Sixteen hours post-transfection, cells were transfected with the helper virus AdNG163R-2[29] at an MOI of 5 and cells were harvested 48 h later. We performed three serial passaging steps using an MOI of 2 of the helper virus AdNG163R-2. According to the published protocol by Palmer and Ng,[29] 31 of 116 cells was grown and amplified as a suspension culture in a spinner culture flask (Bellco Glass, Vineland, NJ) and infected with the lysate of one 150 mm dish from serial passaging step three. Forty-eight hours after infection, cells were harvested and to purify the recombinant vector we performed one CsCl step gradient followed by one equilibrium gradient (20 h, CsCl 1.35 g/cm^3). For buffer exchange, we dialyzed the purified virus in 10 mM Tris (pH 7.5), 10% (v/v) glycerol, and 1 mM $MgCl_2$. DNA sequences contained in the first-generation adenoviral vector fgAdhFIXmg (E1/E3 deleted) and amplification and purification of this recombinant adenoviral vector were described elsewhere.[10]

Titering of helper-dependent vectors. The number of transducing particles contained in the final HD vector preparations was determined as follows: HeLa cells were infected with different volumes of the HD vector preparation. For comparison, HeLa cells were infected at different defined MOIs with the first-generation adenovirus fgAdhFIX[10] to generate a standard curve. Cells were incubated for 3 h and the genomic DNA was isolated followed by a Southern blot probed with either an hFIX cDNA probe (*Hin*dIII/*Eco*RI fragment from plasmid AAV-EF1alpha-F.IX[30]) for pFTC-hFIX-attB-(FRT)2 or a probe containing the left adenoviral inverted terminal repeat with the packaging signal for pFTC-INT-Flp and pFTC-mINT-Flp. The intensity of the bands for the HD vector was compared to the standard curve.

Flp-mediated circle formation from the adenoviral vector genome. To show Flp recombinase–mediated circle formation of the transgene from the adenoviral vector genome, the human hepatoma cell line Huh7 was co-transfected with the gene-deleted adenoviral vectors FTC-INT-Flp and FTC-hFIX-attB-(FRT)2 at a total MOI of 10. Control cells received

either no virus or the previously described first-generation adenovirus fgAdhFIXmg[10] in which the hFIX expression cassette was not split as a positive control. Media were changed daily and the supernatant was analyzed for hFIX expression levels by enzyme-linked immunosorbent assay (ELISA). Four days post-transduction, cells were harvested and genomic DNA isolated to check if Flp-mediated circle formation from the adenoviral vector genome occurred. In brief, after proteinase K digest, a phenol/chloroform extraction was performed followed by ethanol precipitation. A PCR was performed with the primers FTC-240 (5′-ctt gta tgt gtt ggg aat tca tcg-3′) and FTC-547 (5′-gct gtt tgc tgc ttg caa tgt ttg-3′), which are located outside of the FRT sites of the vector pFTC-hFIX-attB-(FRT)2. If the transgene is excised, a 1-kb PCR product will be obtained. To show Flp-mediated excision *in vivo*, genomic DNA was isolated from mouse liver after co-delivery of 1×10^9 TU of the HD vector FTC-hFIX-attB-(FRT)2 and 1×10^9 TU of the second HD vector FTC-INT-Flp encoding Flp and ΦC31.

Cell culture. HeLa cells were maintained in Dulbecco's modified Eagle's medium (Cellgro, Herndon, VA) supplemented with L-glutamine (Gibco BRL, Carlsbad, CA), penicillin/streptomycin (Gibco BRL), and fetal bovine serum (10%). The human hepatoma cell line Huh7 was maintained in Dulbecco's modified Eagle's medium media (Cellgro) supplemented with L-glutamine (Gibco BRL), penicillin/streptomycin (Gibco BRL), nonessential amino acids (Gibco BRL), and fetal bovine serum (10%). For gene-deleted adenoviral production, 116 cells were maintained in minimal essential media (Cellgro) supplemented with L-glutamine (Gibco BRL) and penicillin/streptomycin (Gibco BRL) and fetal bovine serum (10%). First-generation adenovirus was amplified in the human embryonic kidney cell line 293 maintained in Dulbecco's modified Eagle's medium media (Cellgro) supplemented with L-glutamine (Gibco BRL), penicillin/streptomycin (Gibco BRL), and fetal bovine serum (10%).

Animal studies. C57Bl/6 mice (Jackson Laboratories, Bar Harbor, ME) were kept under the Stanford animal facility regulations. C57Bl/6 mice (8–10 weeks old) were injected via high-pressure tail-vein injection as previously described.[25] In brief, the 20 μg plasmid DNA was diluted in 2.0 ml of a physiological 0.9% (w/v) NaCl solution and injected into the mouse tail vein over a time period of 5–7 s. Adenovirus was diluted in Dulbecco's phosphate buffered saline and a total volume of 200 μl Dulbecco's phosphate buffered saline (Gibco BRL). Rapid cell cycling of mouse hepatocytes was induced by injecting CCl_4 intraperitoneally and by performing a surgical two-third partial hepatectomy.

Blood analysis. Mouse serum human FIX antigen levels were determined by ELISA assay as described earlier.[10] The normal human serum level was 5,000 ng/ml. SGPT (alanine aminotransferase activity) assays were performed by using a diagnostic kit for colorimetric determination of SGPT (Sigma procedure no. 505-OP).

Colony-forming assay. To determine the integration efficiencies of linear and circular substrates for ΦC31-mediated integration, a colony-forming assay was performed in HeLa cells. HeLa cells were plated at a density of 5×10^5 cells per 6-cm dish and transfected 24 h later with Superfect (Qiagen). The constructs (C)-pCR-attB-Snori (circular ΦC31 substrate)[25] and (L)-pCR-attB-Snori (linear ΦC31 substrate) for ΦC31-mediated integration were transfected into HeLa cells with the active version of the ΦC31 (ΦC31) integrase or the mutated ΦC31 integrase (m-ΦC31). As a negative control, we co-transfected the linear and circular substrates with "stuffer" DNA derived from the plasmid pBluescript (Stratgene, La Jolla, CA). Both substrates contained the ΦC31 recognition site attB and a neomycin expression cassette for expression in mammalian cells, which allows for cell growth in selective media containing G418. The linear phiC31 substrate was produced by digest of (C)-pCR-attB-Snori with the restriction enzyme endonucleases *Not*I and *Spe*I. For transfection, 2 μg of the linear or circular substrate and the ΦC31 or m-ΦC31 encoding plasmid was transfected. Additional control groups received 2 μg of either the linear or the circular substrate and "stuffer" DNA. Forty-eight hours after transfection, the cells were diluted into 10-cm dishes at a density of either 3.8×10^4 or 3.8×10^5 cells per 10-cm dish. Cells were selected for 14 days with G418-containing media (500 μg/ml). A methylene blue staining was performed and cell colonies counted.

To test if DNA sequences contained in the plasmids pFTC-INT-Flp and pFTC-mINT-Flp are sufficient to integrate substrates for ΦC31-mediated integration, we performed a colony-forming assay. We co-transfected HeLa cells with the plasmid (C)-pCR-attB-Snori and either pFTC-INT-Flp or pFTC-mINT-Flp at a molar ratio of 1:1, respectively. After 2 weeks of G418 selection (500 μg/ml), we performed a methylene blue staining and cell colonies were counted.

Analyses of integration events in mouse liver from a gene-deleted adenoviral vector. For genomic DNA isolation, the mouse liver was removed and homogenized, and a 100-mg portion was used for DNA extraction. Mouse liver genomic DNA was isolated by proteinase K digest followed by phenol/chloroform extraction and ethanol precipitation. The BD GenomeWalker™ Kit from BD Biosciences Clontech was adopted to determine sites of insertion. Four genomic DNA libraries with restriction enzyme nucleases that create blunt-ended DNA fragments (*Dra*I, *Eco*RV, *Pvu*II, *Ssp*I) were produced and a linker was ligated to the DNA fragments. A two-step PCR was performed in which one primer binds to the attB arm and the other primer binds to the linker (primer pair for first PCR: AttB-F, 5′-tac cgt cga cga tgt agg tca cgg tc-3′ and adopter primer 1, 5′-gta ata cga ctc act ata ggg c-3′; primer pair for the nested PCR: AttB-F3, 5′-cga agc cgc ggt gcg-3′ and adopter primer 2, 5′-act ata ggg cac gcg tgg t-3′). PCR products were subcloned and the sequences analyzed.

Detection and characterization of the mpsL1 integration sites in mouse liver. Genomic DNA from mouse liver was isolated and a PCR with the two mpsL1 integration site–specific primers MpsL1 forward (5′-gtg gca cat tcc tta atc cc-3′) and MpsL1 reverse (5′-tga gga gga gcc tta gca ac-3′), which were combined with the attB-specific primer AttB-F (5′-tac cgt cga cga tgt agg tca cgg tc-3′), was performed. This first PCR was followed by a second PCR in which the primer attB-F3 (5′-cga agc cgc ggt gcg-3′) was combined with either MpsL1 forward or MpsL1. To determine the DNA sequences of the resulting PCR products, the DNA fragments were subcloned using a TA-cloning kit (Invitrogen, Carlsbad, CA) and sequenced. As internal control, the interleukin 2 DNA (IL-2) was detected with the following primers: IL-2 5′ (5′-cta ggc cac aga att gaa aga tct-3′) and IL-2 3′ (5′-gta ggt gga aat tct agc atc atc c-3′).

Quantification of genome copy numbers in mouse hepatocytes. To detect the total copy number per cell, a quantitative real-time PCR was performed (GeneAmp® 5700 Sequence Detection System, PE Biosystems, Foster City, CA). Genomic DNA from mouse liver was isolated and 10 ng of liver genomic DNA was analyzed using a SYBR Green kit (PE Biosystems). The following conditions were used: 40 cycles at 95°C for 15 s and 60°C for 1 min. The PCR product is located in the hFIX cDNA (nt 5,032–5,800 from pBS-ApoEHCR(s)-hAATp-hFIXmg-bpA[31]) and for the amplification an hFIX forward primer (5′-aag atg cca aac cag gtc aat t-3′) and an hFIX reverse primer (5′-gat aga gcc tcc aca gaa tgc a-3′) were used. To generate a standard curve, we used 10, 100, 1,000, 10,000, 100,000, and 1,000,000 copies of the plasmid pBS-ApoEHCR(s)-hAATp-hFIXmg-bpA[31] spiked with genomic DNA.

ACKNOWLEDGMENTS

We thank Philip Ng for providing the producer cell line 116 and the helper virus AdNG163R-2 for gene-deleted adenoviral production. This work was supported by NIH Grant DK49022 to MAK and by DFG Grant SFB 455 to AE.

REFERENCES

1. Schroder, AR *et al.* (2002). HIV-1 integration in the human genome favors active genes, local hotspots. *Cell* **110**: 521–529.
2. Hacein-Bey-Abina, S *et al.* (2003). LMO2-associated clonal T cell proliferation in two patients after gene therapy for SCID-X1. *Science* **302**: 415–419.
3. Cavazzana-Calvo, M *et al.* (2000). Gene therapy of human severe combined immunodeficiency (SCID)-X1 disease. *Science* **288**: 669–672.
4. Nakai, H *et al.* (2003). AAV serotype 2 vectors preferentially integrate into active genes in mice. *Nat Genet* **34**: 297–302.
5. Ivics, Z, Hackett, PB, Plasterk, RH and Izsvak, Z (1997). Molecular reconstruction of Sleeping Beauty, a Tc1-like transposon from fish, and its transposition in human cells. *Cell* **91**: 501–510.
6. Yant, SR *et al.* (2005). High-resolution genome-wide mapping of transposon integration in mammals. *Mol Cell Biol* **25**: 2085–2094.
7. Groth, AC and Calos, MP (2004). Phage integrases: biology and applications. *J Mol Biol* **335**: 667–678.
8. Thyagarajan, B, Olivares, EC, Hollis, RP, Ginsburg, DS and Calos, MP (2001). Site-specific genomic integration in mammalian cells mediated by phage phiC31 integrase. *Mol Cell Biol* **21**: 3926–3934.
9. Olivares, EC *et al.* (2002). Site-specific genomic integration produces therapeutic Factor IX levels in mice. *Nat Biotechnol* **20**: 1124–1128.
10. Ehrhardt, A and Kay, MA (2002). A new adenoviral helper-dependent vector results in long-term therapeutic levels of human coagulation factor IX at low doses *in vivo*. *Blood* **99**: 3923–3930.
11. Brunetti-Pierri, N *et al.* (2005). Sustained phenotypic correction of canine hemophilia B after systemic administration of helper-dependent adenoviral vector. *Hum Gene Ther* **16**: 811–820.
12. Chuah, MK *et al.* (2003). Therapeutic factor VIII levels and negligible toxicity in mouse and dog models of hemophilia A following gene therapy with high-capacity adenoviral vectors. *Blood* **101**: 1734–1743.
13. Toietta, G *et al.* (2005). Lifelong elimination of hyperbilirubinemia in the Gunn rat with a single injection of helper-dependent adenoviral vector. *Proc Natl Acad Sci USA* **102**: 3930–3935.
14. Morral, N *et al.* (1999). Administration of helper-dependent adenoviral vectors and sequential delivery of different vector serotype for long-term liver-directed gene transfer in baboons. *Proc Natl Acad Sci USA* **96**: 12816–12821.
15. Picard-Maureau, M *et al.* (2004). Foamy virus–adenovirus hybrid vectors. *Gene Ther* **11**: 722–728.
16. Murphy, SJ, Chong, H, Bell, S, Diaz, RM and Vile, RG (2002). Novel integrating adenoviral/retroviral hybrid vector for gene therapy. *Hum Gene Ther* **13**: 745–760.
17. Lieber, A, Steinwaerder, DS, Carlson, CA and Kay, MA (1999). Integrating adenovirus-adeno-associated virus hybrid vectors devoid of all viral genes. *J Virol* **73**: 9314–9324.
18. Yant, SR *et al.* (2002). Transposition from a gutless adeno-transposon vector stabilizes transgene expression *in vivo*. *Nat Biotechnol* **20**: 999–1005.
19. Soifer, HS and Kasahara, N (2004). Retrotransposon–adenovirus hybrid vectors: efficient delivery and stable integration of transgenes via a two-stage mechanism. *Curr Gene Ther* **4**: 373–384.
20. Soifer, H *et al.* (2002). A novel, helper-dependent, adenovirus-retrovirus hybrid vector: stable transduction by a two-stage mechanism. *Mol Ther* **5**: 599–608.
21. Chen, ZY *et al.* (2001). Linear DNAs concatemerize *in vivo* and result in sustained transgene expression in mouse liver. *Mol Ther* **3**: 403–410.
22. Thorpe, HM and Smith, MC (1998). *In vitro* site-specific integration of bacteriophage DNA catalyzed by a recombinase of the resolvase/invertase family. *Proc Natl Acad Sci USA* **95**: 5505–5510.
23. Hillgenberg, M *et al.* (2001). Chromosomal integration pattern of a helper-dependent minimal adenovirus vector with a selectable marker inserted into a 27.4-kilobase genomic stuffer. *J Virol* **75**: 9896–9908.
24. Ohbayashi, F *et al.* (2005). Correction of chromosomal mutation and random integration in embryonic stem cells with helper-dependent adenoviral vectors. *Proc Natl Acad Sci USA* **102**: 13628–13633.
25. Ehrhardt, A, Xu, H, Huang, Z, Engler, JA and Kay, MA (2005). A direct comparison of two nonviral gene therapy vectors for somatic integration: *in vivo* evaluation of the bacteriophage integrase phiC31 and the Sleeping Beauty transposase. *Mol Ther* **11**: 695–706.
26. Chalberg, TW *et al.* (2006). Integration specificity of phage phiC31 integrase in the human genome. *J Mol Biol* **357**: 28–48.
27. Recchia, A, Perani, L, Sartori, D, Olgiati, C and Mavilio, F (2004). Site-specific integration of functional transgenes into the human genome by adeno/AAV hybrid vectors. *Mol Ther* **10**: 660–670.
28. Groth, AC, Olivares, EC, Thyagarajan, B and Calos, MP (2000). A phage integrase directs efficient site-specific integration in human cells. *Proc Natl Acad Sci USA* **97**: 5995–6000.
29. Palmer, D and Ng, P (2003). Improved system for helper-dependent adenoviral vector production. *Mol Ther* **8**: 846–852.
30. Nakai, H *et al.* (1998). Adeno-associated viral vector-mediated gene transfer of human blood coagulation factor IX into mouse liver. *Blood* **91**: 4600–4607.
31. Miao, CH *et al.* (2000). Inclusion of the hepatic locus control region, an intron, and untranslated region increases and stabilizes hepatic factor IX gene expression *in vivo* but not *in vitro*. *Mol Ther* **1**: 522–532.